Some Fractographic Features of Various Weld Cracking and Fracture Surfaces with Scanning Electron Microscope†

—Studies on Fractography of Welded Zone (I)—

Fukuhisa MATSUDA* and Hiroji NAKAGAWA**

Abstract

Typical examples of various weld cracked and fractured surfaces, that is, solidification crack, liquation crack, hydrogen-induced crack, lamellar tear, quenching crack, fatigue fracture and others are displayed and classified with scanning electron microscope. Moreover some fractographic features are investigated with the aid of microanalyzer.

1. Introduction

Since various weld crackings during and after welding and fractures of welded joint which are classified as shown in **Table 1** are one of the serious problems related to welding, many researches have been performed to make clear the causes and to develope the prevention methods of these problems. Hitherto most of the techniques of the investigation for the causes has been mainly limited to; (1) estimation of the position, temperature and environment where the crack and/or the fracture occurred, (2) observation of the microstructure near the crack and/or fracture with an optical microscope, (3) observation of the degree of brilliance and oxidization of the cracked and/or fractured surface with a naked eye or a microstereoscope, etc.

Recent years the microfractography has been developed with the advance of electron microscopy, and thus the relation between the cause or mode of the fracture and the microfeature of the fractured surface has gradually become clear. The typically basic relations are shown in **Table 2.** Such systematization of these rela-

Table 1 Classification of weld crackings and fractures

Weld cracking in welding performance	Hot cracking	Solidification cracking
		Liquation cracking
		Ductility-dip cracking
	Cold cracking	Hydrogen cracking (Delayed cracking)
		(Lamellar tearing)
		Quenching cracking during Martensitic transformation
	Reheat cracking	
Weld cracking and fracture in service	(Overload fracture)	
	Brittle fracture	
	Fatigue fracture	
	Environmental fracture	Stress corrosion cracking
		Corrosion fatigue
		etc.
	Creep fracture	
	etc.	
Other defect	Blow hole	
	Lack of fusion	
	Slag inclusion	

† Received on March 30, 1977

* Professor

** Research Instructor

Table 2 Relation between basic fracture mode and microfeature of fractured surface

Transgranular fracture	Ductile fracture	
	Microvoid coalescence	Dimple(Equiaxed, Shear, Tear dimple)
	Glide plane decohesion	Serpentine glide, Ripple, Stretching
	Brittle fracture	
	Cleavage fracture	River pattern, Tongue
	Quasi-cleavage fracture	River pattern, Tear ridge
	Fatigue fracture	Striation, Tire track, Rub mark
Intergranular fracture	Ductile fracture	Separated grain facet, surface of which shows dimples
	Brittle fracture	Separated grain facet, surface of which is flat
	Fatigue fracture	Separated grain facet, surface of which shows striations

tions must enable the researchers to obtain various and important informations about the cause of the fracture.

Therefore the microfractographic technique has been gradually applied to the fracture analysis of welded joint. As is generally known, however, a welded zone is generally suffered under a metallurgically and mechanically complicated condition. This causes a complicated fracture mode and thus a complicated fracture surface. This means that the individual and the mutual effects of the various factors must be especially taken into account for the establishment of the weld microfractography. Moreover the features of blowhole, lack of fusion, slag inclusions and etc. on the fractured surface must be clear, since they have a possibility to become nucleation sites of a huge fracture.

From these viewpoints the authors have been investigating the various cracked and fractured surfaces in welded joint. For the observation a scanning electron microscope (SEM, HITACHI HSM-2B type), which was set up in 1975, has been used, the general view of which is shown in **Photo. 1.** The magnification is continuously variable from $\times 12$ up to $\times 100{,}000$. Moreover this SEM contains two kinds of microanalyzer. One is a wave dispersive type analyzer (EPMA) composed of two channels and six analyzing crystals, with which analysis from boron to uranium is possible. The other is an energy dispersive type analyzer (EDX), with which analysis from sodium to uranium is possible. These microanalyses offer very important information for the fracture analyses.

This report describes the outline of various weld cracked and fractured surfaces, using typical examples.

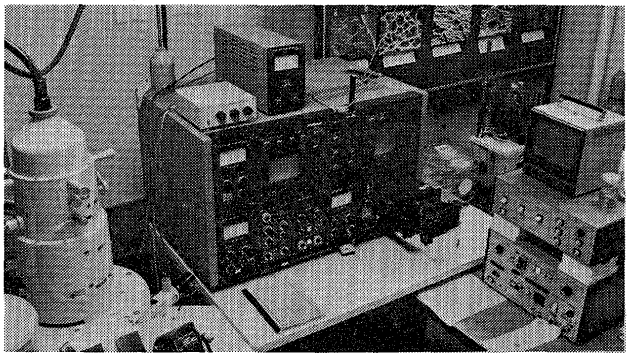

Photo. 1 General appearance of the scanning electron microscope in JWRI

2. Examples of Weld Cracking and Fractured Surfaces

2.1 Hot Cracking

2.1.1 *Solidification Crack*

Photograph 2 shows a solidification cracked surface of fully austenitic stainless steel of SUS310S* tested with Trans-Varestraint method. One of the merit of this testing method is to be able to determine the relation between the each location in the crack and its temperature during welding, since the crack occurs instantaneously. In Photo. 2 the temperature is lowered from the left toward the right side. The cracked surface as a whole shows a feature of intergranular cracking which is elongated unidirectionally due to the columnar growth. The detail, however, changes from the higher temperature region to the lower temperature region. That is, in the region at the highest tem-

* SUS310S corresponds to AISI310S. SUS is the designation for stainless steel in Japan Industrial Standard (JIS).

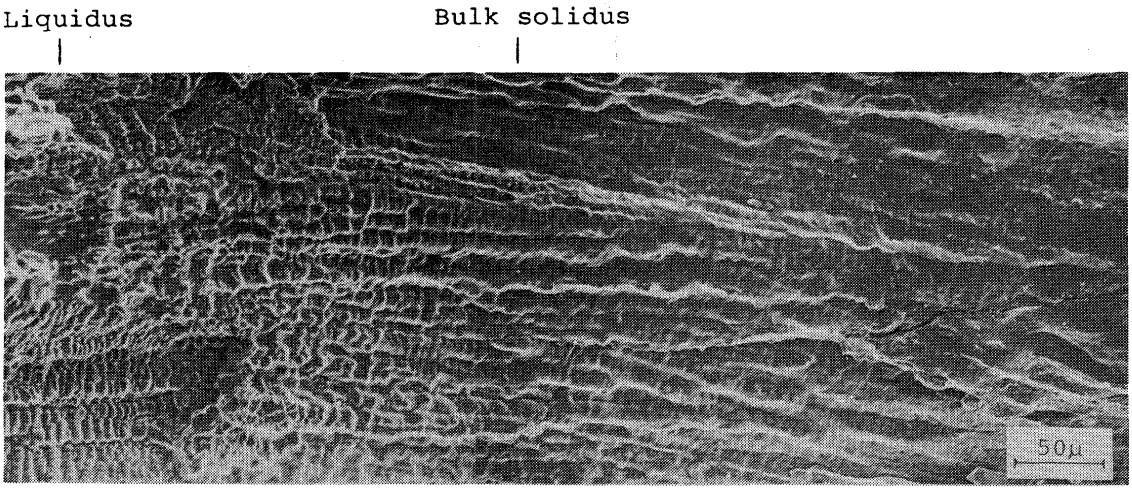

Photo. 2 Solidification cracked surface of SUS310S occurred with Trans-Varestraint test

perature many and fine protuberances are remarkably observed, which correspond to the primary and secondary arms of cellular dendrites. In the region at the medium temperature the protuberances of secondary arms gradually become obscure. Further, in the region at the lowest temperature the protuberances of primary arms also become obscure, and a flat surface becomes dominant. The reason of such a change is mainly because of the decrease in the residual liquid together with the temperature drop, and partly because of the grain boundary migration among residual low melting liquids in the lowest temperature region[1].

Similar cracked surface is also observed for a weld solidification crack of aluminum alloy[2]. It is, however, doubtful in aluminum alloy whether the grain boundary migration affects or not.

Using this feature, it is possible to estimate the cracked temperature during welding of any specimen tested with another cracking test or in actual welding performance. For example **Photo. 3** shows a solidification cracked surface of aluminum alloy 5083 tested with Houldcroft type method. Though the cracked surface shows a non-directional intergranular cracking due to the equiaxed crystals, many protuberances are remarkably observed. Therefore it is considered that the crack occurred near the liquidus temperature. The authors confirmed this by photographing the tip of solidification cracking with 16 mm movie camera. Moreover the cracked surface near the arrested location of the cracking in this specimen was similar to that in the lowest temperature region in Photo. 2.

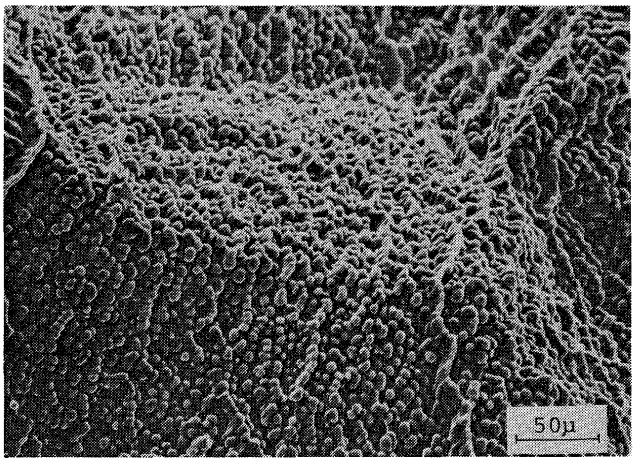

Photo. 3 Solidification cracked surface of 5083 aluminum alloy occurred with Houldcroft type test

2.1.2 *Liquation Crack*

For an example, a liquation cracked surface of a heat-affected zone of SUS310S is shown in **Photo. 4.**

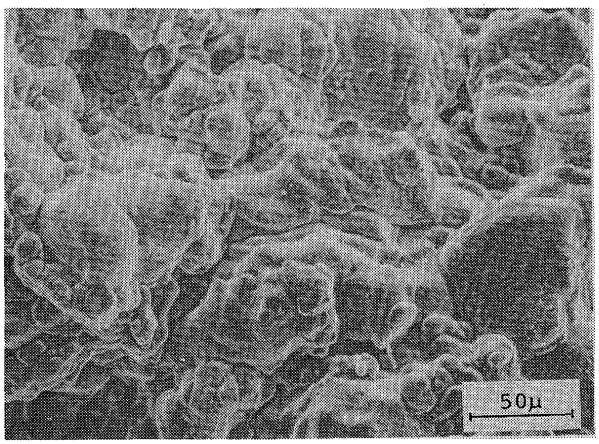

Photo. 4 Liquation cracked surface in HAZ of SUS310S

The cracked surface shows a feature of intergranular cracking, but gives an rounded appearance compared with that in cold cracking mentioned later. Besides, in Photo. 4 some protuberances which are somewhat similar to those of dendrites are observed. Since the location of Photo. 4 is an extreme vicinity of the

fusion boundary, it is considered that these protuberances mean the existence of much liquid among the grain boundaries during welding.

2.1.3 *Ductility-dip Crack*

In SUS310S tested with Trans-Varestraint method, ductility-dip cracks occur between about 1200°C–850°C. The cracked surface also shows a feature of intergranular cracking as shown in **Photo. 5***, but the

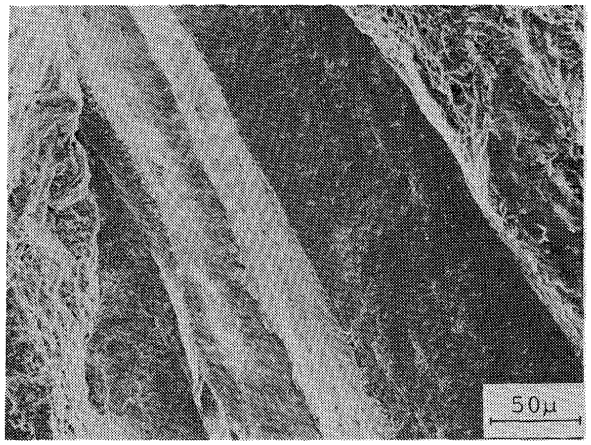

Photo. 5 Ductility-dip cracked surface in weld metal of SUS310S occurred with Trans-Varestraint test

ridge of the grain boundary is seemed to be somewhat sharper than that in the lowest temperature region in Photo. 2. Besides the cracked surface looks slightly rough in higher magnification. Moreover the ductility-dip cracked surface differs from the solidification cracked surface in their element distributions. On the solidification cracked surface the elements such as sulphur forming low melting products are often observed. On the ductility-dip cracked surface, however, carbon which may form carbide of $M_{23}C_6$ type was detected.

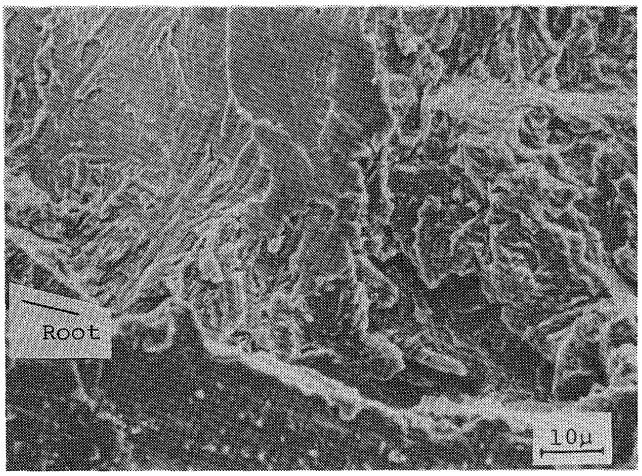

(a) vicinity of the root

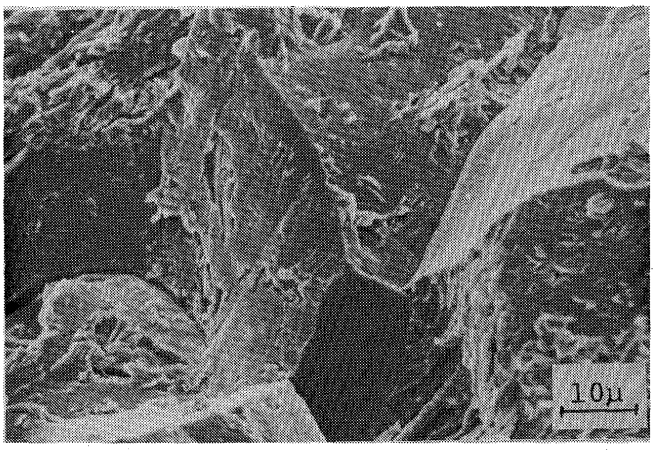

(b) coarse grained region near fusion boundary

Photo. 6 Root cracked surface in HAZ occurred with y-groove cracking test. material; HT50 (40 mm thickness), electrode; JIS D5016 (diffusible hydrogen; 4 cc/100 g), heat input; 22,000 J/cm, non-preheating

2.2 Cold Cracking

2.2.1 *Hydrogen-Induced Crack*

(a) Root Crack

It is shown[3] that the root crack in the y-groove cracking test generally originates in the heat-affected zone and propagates into the weld metal. The cracked surfaces in both the heat-affected zone and the weld metal are composed of either intergranular, quasi-cleavage, dimple, or their two or three mixed fracture mode. **Photograph 6(a)** shows an example of the quasi-cleavage fracture mode in heat-affected zone. Since in any welded zone the evaluation of the stress intensity factor and the hydrogen concentration at each crack tip is impossible at present, the systematic description of the distribution of fracture mode in the cold cracked surface is difficult. Despite this circumstance, intergranular fracture mode is often observed in the coarse grained region of the heat-affected zone as shown in **Photo. 6(b)**.

Besides, in most weld metal not only the intergranular mode but also the quasi-cleavage and dimple modes have often a directional appearance due to an elongated prior austenite grain. An example of this is shown in **Photo. 7.**

Photograph 8 shows a fractured surface near the notch of an Implant tested specimen, in which the intergranular and the quasi-cleavage fracture modes are clearly observed.

* In Photo. 5 the left part and the upper right part are the artificially fractured region showing dimples.

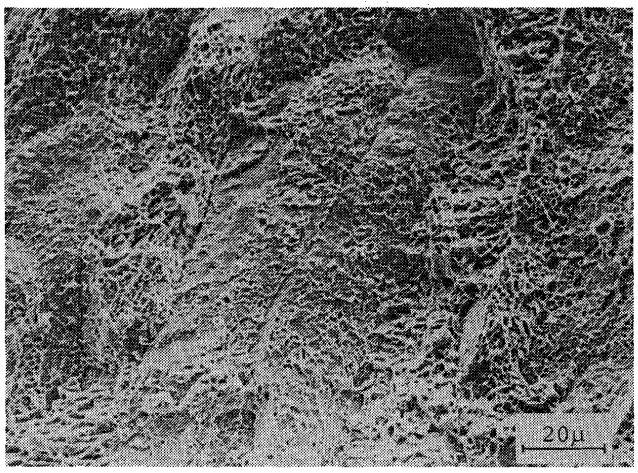

Photo. 7 Root cracked surface in weld metal occurred with Controlled restraint fillet weld cracking test[4]. material; HT80 (25 mm thickness), electrode; E11016 (hydrogen; 20 cc/100 g), heat input; 17,000 J/cm, non-preheating

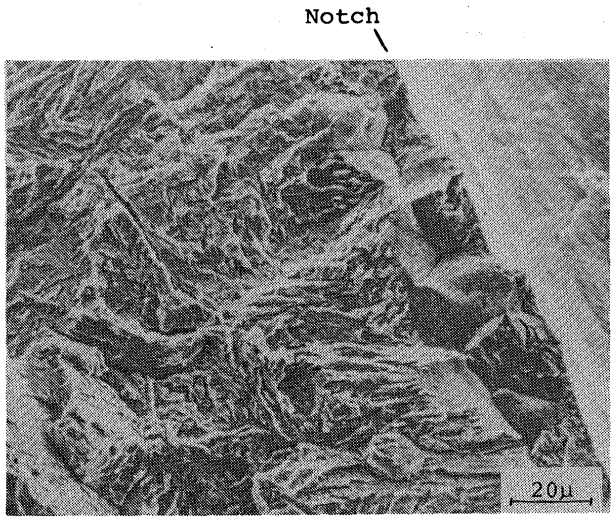

Photo. 8 Root cracked surface near the notch occurred with Implant cracking test. material; HT80, electrode; E11016 (hydrogen; 2 cc/100 g), applied stress; 70 kg/mm² heat-input; 17,000 J/cm, non-preheating

(b) Heel Crack

A heel cracked surface at a extreme vicinity of the root in HT50 (high tensile steel more than 50 kg/mm² in ultimate strength) with Non-restraint T type cracking test[5] shows a quasi-cleavage or fine dimple fracture mode, both of which are affected by hydrogen. An example of the fine dimple fracture mode is shown in **Photo. 9(a)**. **Photograph 9(b)**, whose abscissa is X-ray energy and the ordinate is the intensity, is the EDX result of an inclusion A in a dimple in Photo. 9(a), and this shows the existence of Si, Ca, Mn and Fe. Since the large quantity of Fe is considered to be due to an effect of the matrix judging from the resolving power of EDX, the inclusion must be an oxide composed of Si, Ca and Mn. Moreover the existence of Si and Ca which are the slag constituents may suggest that the heel crack at the extreme vicinity of the root is passing through the weld metal.

Except the extreme vicinity of the root, the cracked surface is composed of a mixture of intergranular and quasi-cleavage fracture mode, as shown in **Photo. 9(c)**. By the way, the sulphur content of this HT50 is 0.009% and thus the inlcusions which were mainly composed of manganese sulphides elongated along the rolling direction were sometimes observed as shown in **Photo. 9(d)**.

On the other hand, in a heel crack of another HT50 containing 0.018% sulphur, a cracked surface as shown in **Photo. 10(a)** was sometimes observed, which is similar to the terrace and wall type in a lamellar tear. Moreover, a cracked surface where many and flat manganese sulphides were clustered together as shown in **Photo. 10(b)** was often observed, although the major cracked surface was the same as in Photo. 9(c).

2.2.2 *Lamellar tearing*

Photograph 11(a) shows a lamellar tearing occurred from a root in a corner joint of HT50 (40 mm thickness, 0.018% sulphur), and this is the typical example of the terrace and wall type reported by Elliot et al[6]. That is, the terrace part shows an equaixed dimple fracture mode in which manganese sulphides along the rolling plane are mainly observed, and the wall part shows a shear dimple mode. Near the root, however, the wall part and the intermediate zone between the adjacent manganese sulphides on the terrace part occasionally show a quasi-cleavage fracture affected by hydrogen, which is similar to Photo. 10(a).

Photograph 11(b) shows another example of the lamellar tearing which occurred at a distance of about 15 mm from the fision boundary in the same joint as in Photo. 11(a). This is somewhat similar to the terrace and wall type, but the terrace part shows a feature of flat seperation between the matrix and the manganese sulphide. The reason may be that there are lots of large manganese sulphides in the nearer position to the thickness center. Though obscure in Photo. 11(b), the large and flat manganese sulphides are often observed on the terrace parts.

By an application of the Implant cracking test of the thickness direction without notch to the above mentioned HT50, a lamellar tearing easily occurred at a distance of about 12 mm from the fusion boundary. The fractured surface is shown in **Photo. 12(a)**, which is similar to Photo. 11(b). The lower portion of Photo. 12(a) is the wall part composed of shear

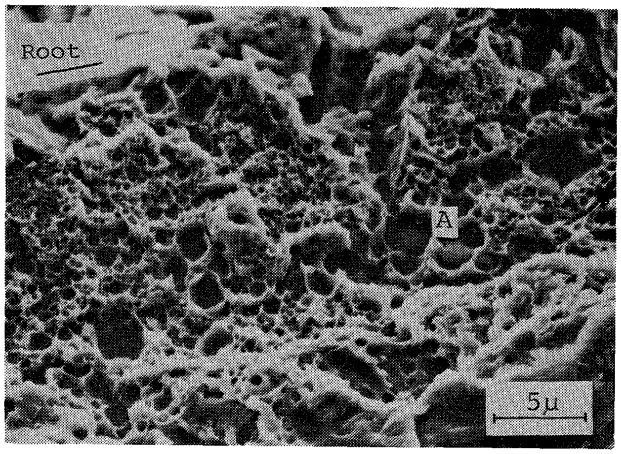

(a) vicinity of the root

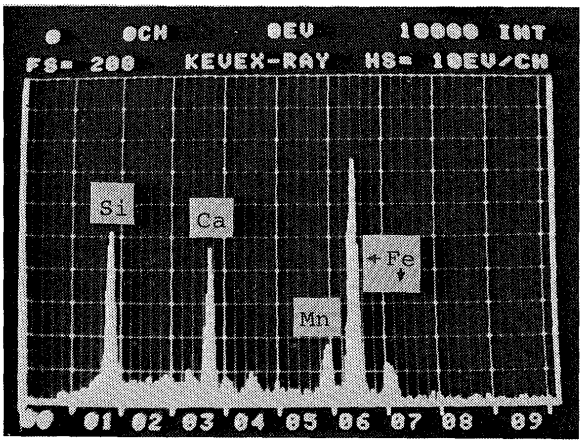

(b) EDX result of inclusion A in (a)

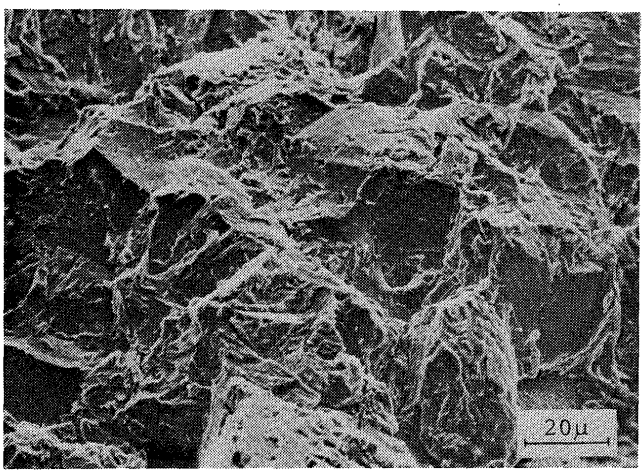

(c) general feature

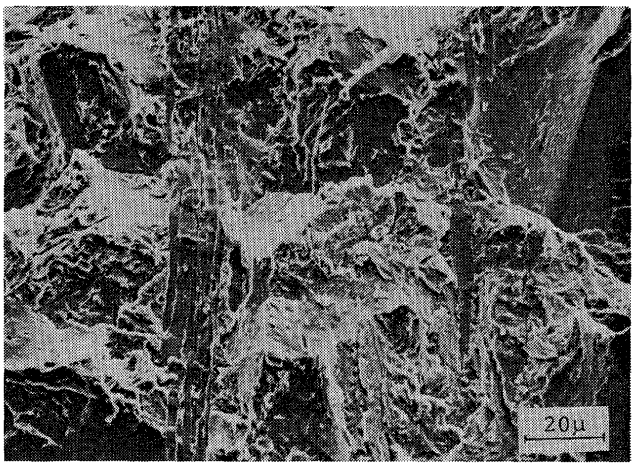

(d) elongated manganese sulphides on the cracked surface

Photo. 9 Heel cracked surface occurred with Non-restraint *T* type cracking test[5]. material; HT50 (16 mm thickness), electrode; D5016 (hydrogen; 4 cc/100 g), heat input; 17,000 J/cm, non-preheating

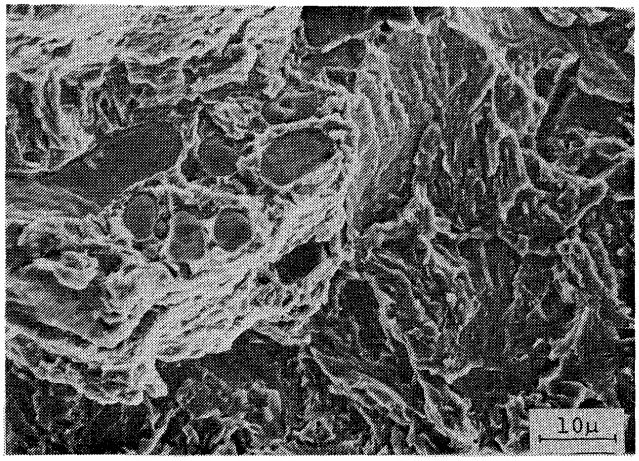

(a) cracked surface as a lamellar tearing

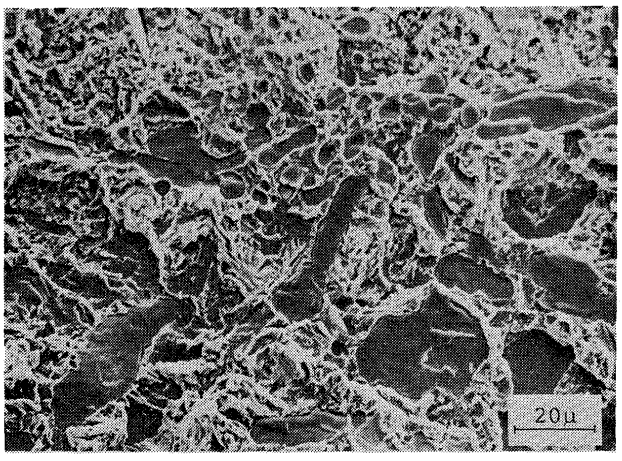

(b) cracked surface where manganese sulphides are clustered

Photo. 10 Another example of heel cracked surface. material; HT50 (40 mm thickness), other conditions are the same as in Photo 9.

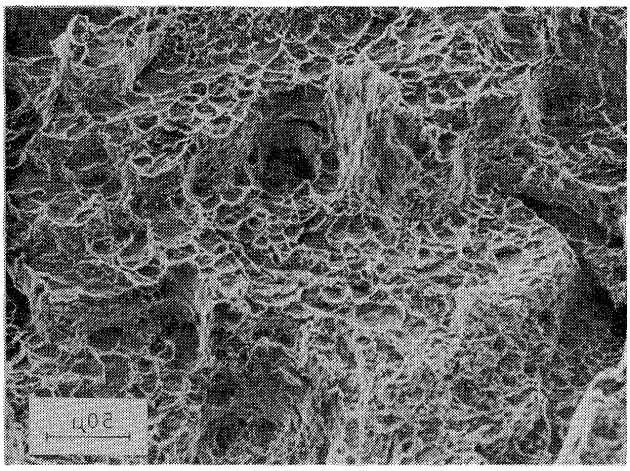

(a) typical terrace and wall type

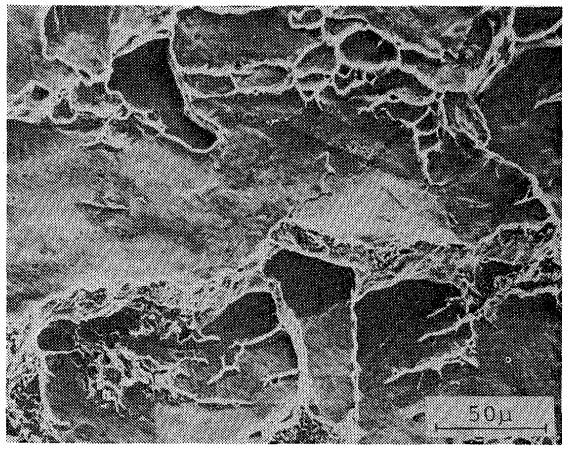

(b) another feature of terrace and wall type

Photo. 11 Lamellar teared surface occurred in a corner joint. material; HT50 (40 mm thickness), electrode; D5016

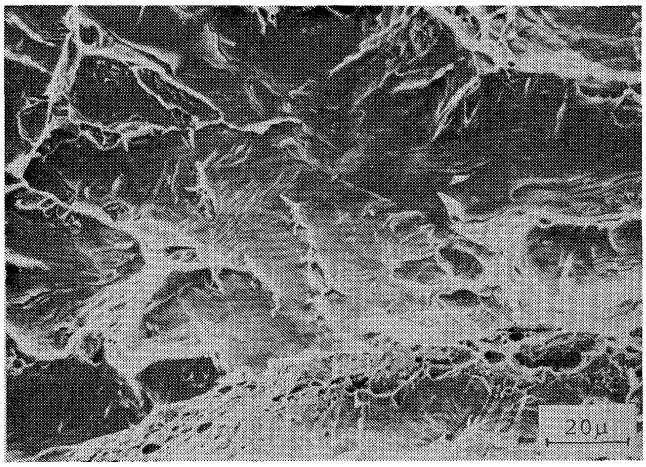

(a) secondary electron image

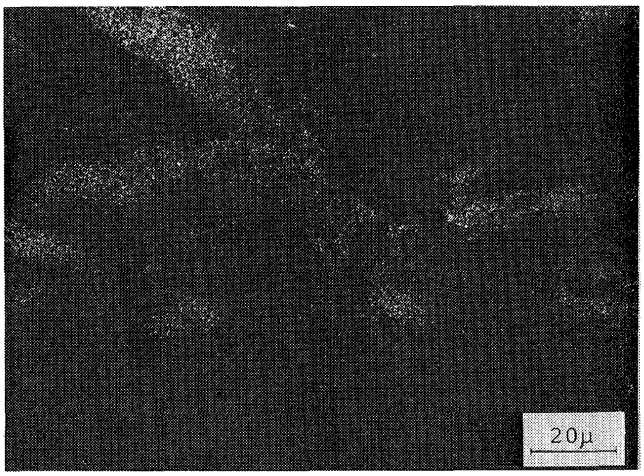

(b) sulphur characteristic X-ray image of (a)

Photo. 12 Lamellar teared surface occurred with Implant cracking test of thickness direction without notch. material; HT50 (same as in Photo 11), electrode; D5016 (hydrogen; 4 cc/100 g), applied stress; 40 kg/mm², heat input; 17,000 J/cm, non-preheating

dimples, and the other portion is the terrace part. The bright lines in the terrace part are the tear ridges between matrices, and the other part shows a flat separation between the matrix and the inclusion. **Photo. 12(b)** is the sulphur characteristic X-ray image of Photo. 12(a), from which the distribution of mangansee sulphides is distinctly observed.

2.2.3 *Quenching Crack during Martensitic Transformation*

It was reported by Kobayashi et al.[7] that another type of cold cracking, that is, a kind of quenching crack during martensitic transformation occurs in hardenable steels. **Photograph 13** shows a toe crack in a SAE4340 steel occurred by the same method as Kobayashi et al[7]. **Photograph 14** shows a similar crack occurred in an electron beam weld metal of a high carbon bearing steel (JIS SUJ2). In both cracked surface, intergranular fractures are mainly observed, though transgranular fractures are partly observed.

2.3 Reheat Cracking

When HT80 specimen of y-groove cracking test which was conducted in the environmental and welding conditions free from hydrogen-induced crack was annealed at 600 °C as the stress-relief, a stress-relief crack readily occurred. **Photograph 15** shows the surface which is a typical intergranular fracture. The cracked surface of the specimen annealed for long duration was severely oxidized, and the feature of the intergranular fracture becomed obscure.

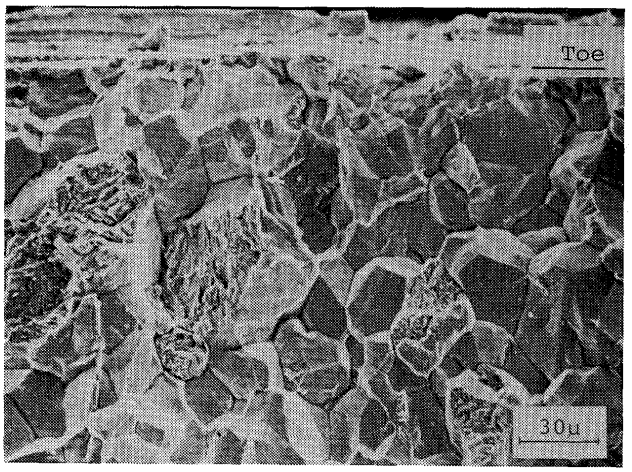

Photo. 13 Toe cracked surface occurred in SAE4340 steel welds. thickness; 25 mm, electrode; D5016 (hydrogen; 4 cc/100 g), heat input; 25,000 J/cm, non-preheating, water quenched just after welding

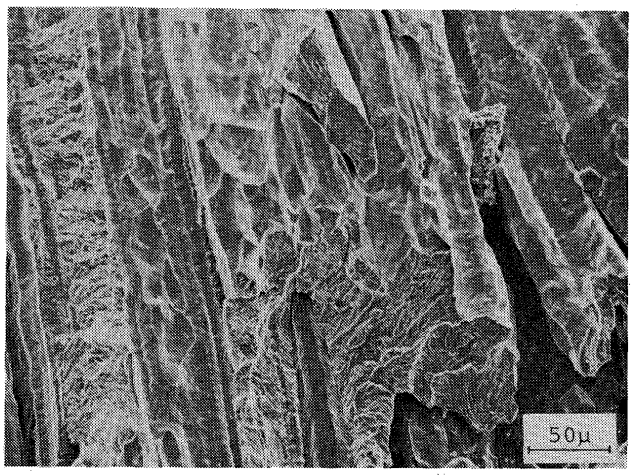

Photo. 14 Cracked surface occurred in electron beam weld metal of SUJ2 bearing steel. thickness; 30 mm, welding condition; 150 kV, 40 mA, 1,000 mm/min

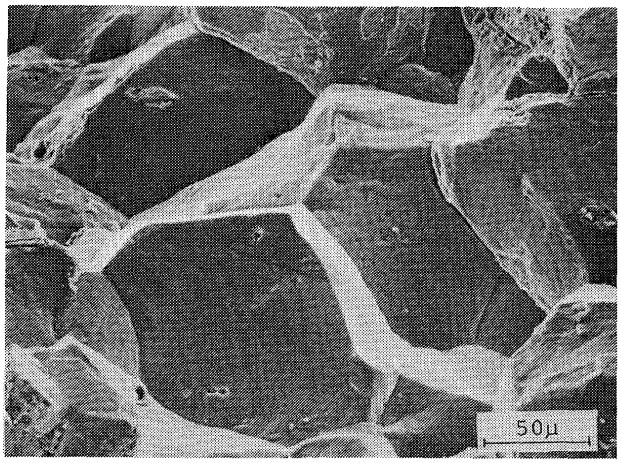

Photo. 15 Stress-relief cracked surface occurred in HT80. electrode; E11016, heat input; 17,000 J/cm, annealing temperature; 600°C

Photograph 16 shows an example of the cracked surface of a Ni-Cr-Mo low alloy steel which was overlayed with a stainless steel electrode and then annealed at 620°C as the stress-relief. This crack is called as under-clad crack in Japan. The cracked surface also shows the intergranular fracture, and the observation of a higher magnifiaction often revealed many and small voids as seen in Photo. 16(b).

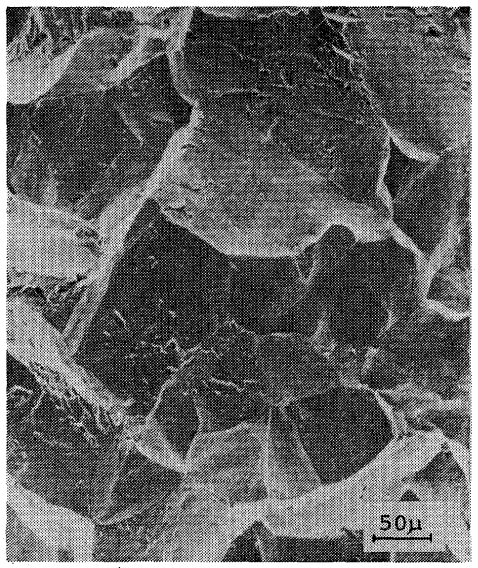

(a) lower magnification

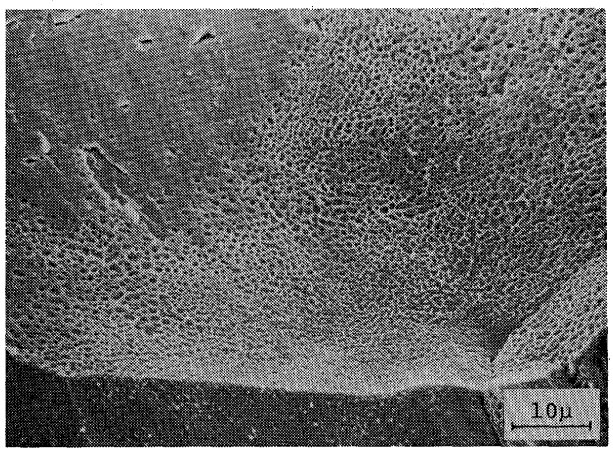

(b) higher magnification

Photo. 16 Under-clad cracked surface occurred in Ni-Cr-Mo low alloy steel overlayed with stainless steel electrode, annealing temperature; 620°C

2.4 Blowhole

Many and small blowholes were sometimes observed on a fatigue fracture surface of MIG weld metal of aluminum alloy, as shown in **Photo. 17(a)**. The observation of a higher magnification revealed a feature of dendritic protuberances inside the blowhole, as shown in **Photo. 17(b)**. The feature of blowholes of another materials was the same.

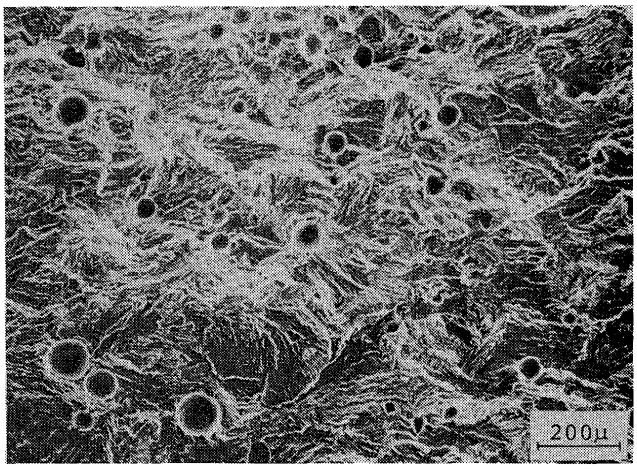

(a) lower magnification

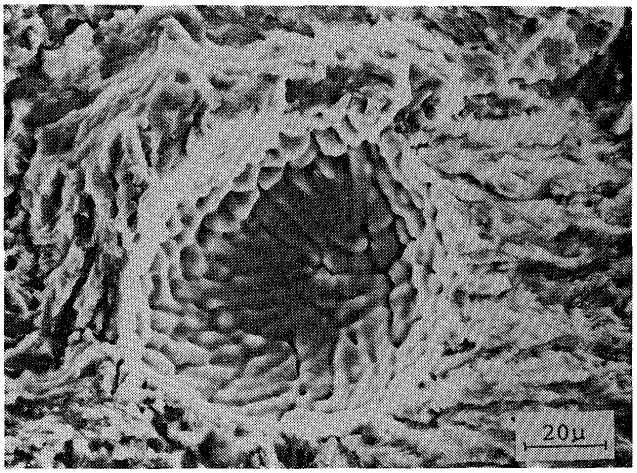

(b) higher magnification

Photo. 17 Blowhole observed on a fatigue fractured surface of 5083 aluminum alloy welds

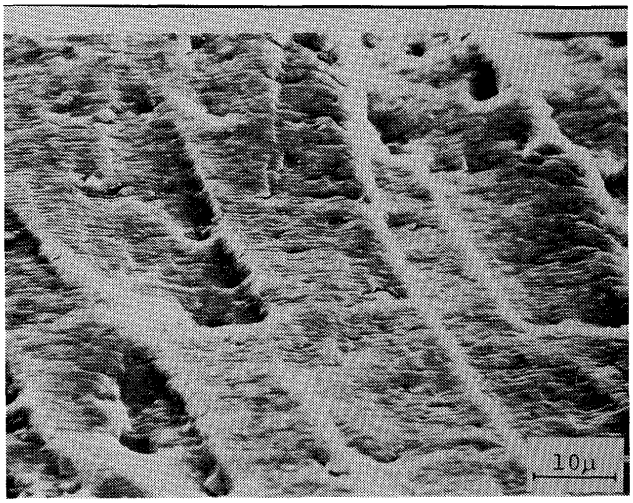

(a) plateau and striation

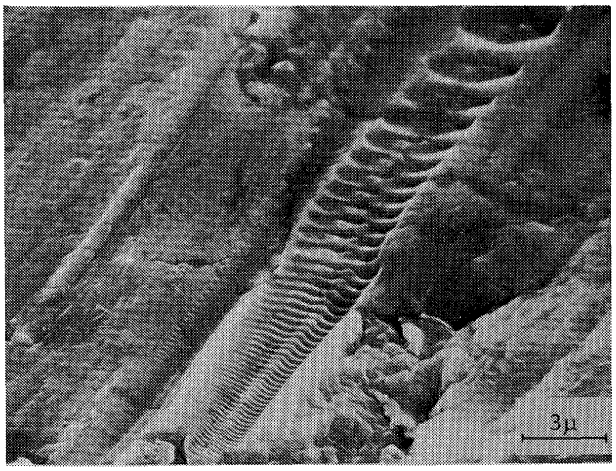

(b) tire track and rub mark

Photo. 18 Fatigue fractured surface of 5083 aluminum alloy weld metal. testing method; Schenck bending type, electrode; 5183, stress; 10 kg/mm^2, N; 2.6×10^5

2.5 Fatigue Fracture

An example of a fatigue fracture of MIG weld metal of aluminum alloy 5083 is shown in **Photo. 18**. Photograph 18(a) shows typical striations on plateaus, and Photo. 18(b) shows a tire track and rub mark which are another evidence of a fatigue fracture.

Photograph 19 shows a fatigue fracture near a toe of electron beam welds of HT50 which occurred from the toe of welds. Major fracture surface was perhaps a kind of cleavage fracture as seen in Photo. 19(a), and an intergranular fracture was sometimes observed as seen in Photo. 19(b).

2.6 Stress Corrosion Cracking

Photograph 20(a) and **(b)** respectively show the examples of stress corrosion cracking in heat-affected zone and weld metal of aluminum alloy (JIS 7N01), and both show intergranular features.

3. Summary

Some typical examples of various cracked and fractured surfaces were shown in this introductory report, but as indicated above there remain many unknown problems. Each detail shall be published hereafter by the authors as the investigation proceeds.

The authors would like to thank many industries for their offering samples and Mr. K. Tohmoto for his assistance.

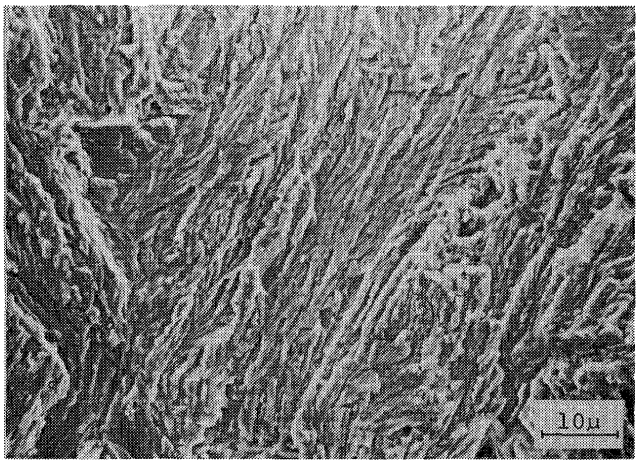

(a) cleavage-like fractured surface

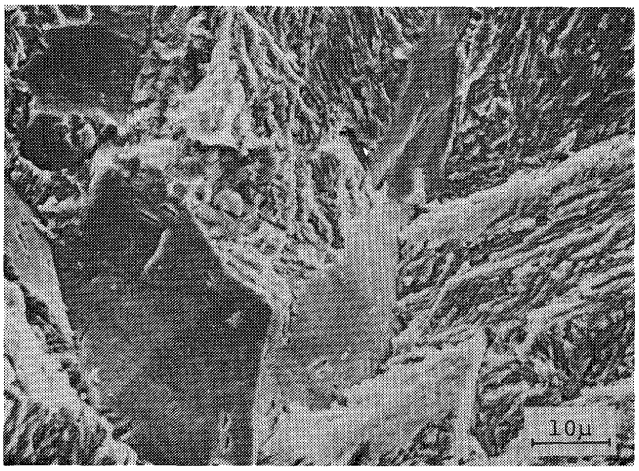

(b) intergranular fractured surface

Photo. 19 Fatigue fractured surface near toe part of HT50 electron beam welds. testing method; Schenck bending type, stress; 18 kg/mm², N; 7.5×10^5

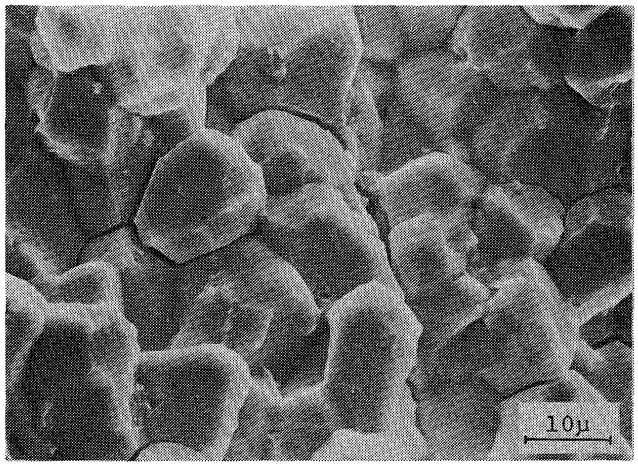

(a) HAZ

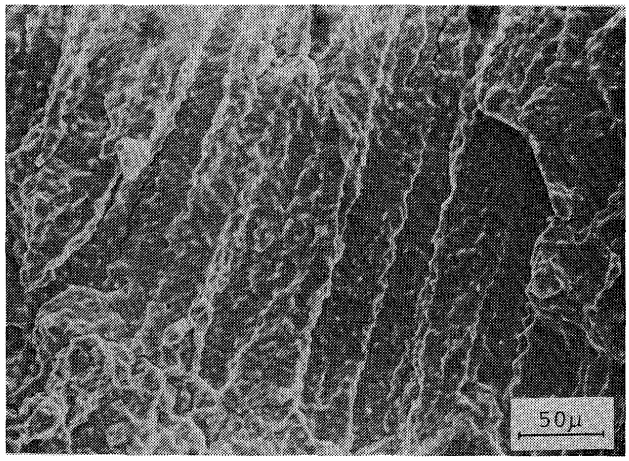

(b) weld metal

Photo. 20 Stress corrosion cracked surface of 7N01 aluminum alloy welds. electrode; 5556, corrosive agent; chromate saline solution, stress; 75% of the proof stress

References

1) F. Matsuda, et al: to be published.
2) Y. Arata, et al.: Trans. JWRI., Vol. 5 (1976), No. 2. p. 154.
3) H. Kihara, et al.: J. Japan Weld. Soc., Vol. 31 (1962), No. 1, p. 53 (in Japanese)
4) J. Tsuboi, et al.: J. Japan Weld. Soc., Vol. 43 (1974), No. 10, p. 1038 (in Japanese)
5) H. Kihara, et al.: J. Japan Weld. Soc., Vol. 39 (1970), No. 3, p. 156 (in Japanese)
6) D. N. Elliot: Met. Const. & British Weld. J., Vol. 1 (1969), p. 50.
7) T. Kobayashi, et al.: Trans. JWS., Vol. 2 (1971), No. 1, p. 70.